JACS
JOURNAL OF THE AMERICAN CHEMICAL SOCIETY
Article
pubs.acs.org/JACS

Using Molecular Architecture to Control the Reactivity of a Triplet Vinylnitrene

Sujan K. Sarkar,[†] Onyinye Osisioma,[†] William L. Karney,[‡] Manabu Abe,[§] and Anna D. Gudmundsdottir*[,†]

[†]Department of Chemistry, University of Cincinnati, Cincinnati, Ohio 45221, United States

[‡]Department of Chemistry and Department of Environmental Science, University of San Francisco, 2130 Fulton Street, San Francisco, California 94117, United States

[§]Department of Chemistry, Graduate School of Science, Hiroshima University, Hiroshima 739-8526, Japan

Supporting Information

ABSTRACT: Photolysis of 3-azido-1-indenone (**1**) with a light-emitting diode (LED, λ = 405 nm) or mercury arc lamp (Pyrex) resulted in the formation of heterodimer **3** in excellent yield, through dimerization of triplet vinylnitrene ^{3}**2**. At ambient temperature, vinylnitrene ^{3}**2** (λ_{max} at 340 and 480 nm) was detected directly with laser flash photolysis of vinyl azide **1**. The vinylnitrene intermediate was also characterized directly with IR and ESR spectroscopy in cryogenic matrices. The ESR spectrum of vinylnitrene ^{3}**2** yielded a zero-field splitting parameter $|D/hc|$ of 0.460 cm^{-1} and $|E/hc|$ of 0.015 cm^{-1}, which reveals that vinylnitrene ^{3}**2** has significant 1,3-biradical character. The proposed mechanism for the formation and reactivity of triplet vinylnitrene ^{3}**2** was supported with density functional theory (DFT) calculations, which highlight that the steric demand of the five-membered ring in vinylnitrene ^{3}**2** prevents intersystem crossing to the corresponding azirine (**10**). CASSCF and CASPT2 calculations showed that the energy gap between the singlet and triplet configurations of vinylnitrene **2** is only 10 kcal/mol. In spite of this small energy gap, vinylnitrene ^{3}**2** does not decay by intersystem crossing, but rather by dimerization. Thus, triplet vinylnitrenes can be selectively formed with visible light and used to form new C−N bonds in synthetic applications.

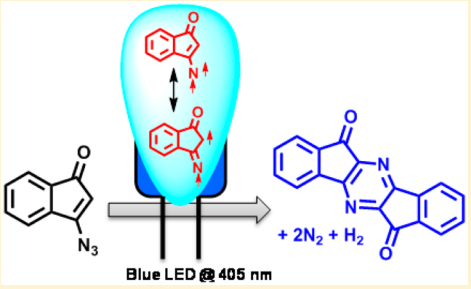

INTRODUCTION

Organic azides are one of the more versatile building blocks in synthetic chemistry because they react readily with both electrophiles and nucleophiles to form new C−N bonds.[1] The dipolar nature of organic azides makes them suitable for cycloaddition to alkynes and olefins, which has been used in countless syntheses.[2] Furthermore, the quest for sustainable chemistry has sparked interest in using sunlight, a natural resource, or energy-efficient light-emitting diodes (LED) for synthetic applications. Most organic azides do not absorb visible light; nevertheless, with the aid of transition metal photocatalysts, they can undergo photochemical transformation with visible light.[3] For example, photocatalytic sensitization of vinyl azides has been successfully used for selective C−N bond formation.[4] However, photolyses of organic azides have limited use in synthesis, as direct irradiation of azides generally yields nitrenes, which are electron-deficient, nitrogen-centered biradicals[5,6] with limited selectivity in bimolecular reactions. The reactivity of nitrenes depends on the molecular architecture, including the electron configuration and substituents. Although electron-donating substituents, such as aryl-, alkyl-, and vinyl-groups, stabilize nitrene intermediates, they influence nitrene reactivity differently. For example, direct photolysis of aryl azides with bulky *ortho*-substituents yields singlet arylnitrenes that are long-lived enough to insert indiscriminatingly into surrounding bonds.[5,7] Thus, they have been used in applications such as photoaffinity labeling[7,8] and cross-linking in materials science (Scheme 1).[9−12] Singlet arylnitrenes without *ortho*-substituents are short-lived and decay by intramolecular reactivity. In contrast, triplet arylnitrenes are generally long-lived intermediates that decay mainly by dimerization.[13,14] They are stable at cryogenic temperature and have been detected directly with UV, IR, and ESR spectroscopy. Triplet arylnitrenes can be formed either by intersystem crossing of singlet nitrenes or by triplet sensitization of aryl azides.

In comparison, direct irradiation of alkyl azides does not yield singlet alkylnitrenes, but imine products in a concerted manner from their singlet excited state. However, triplet sensitization of alkyl azides yields alkylnitrenes that decay by dimerization (Scheme 2).[15,16] Triplet alkylnitrenes are also stable at cryogenic temperature and have been characterized directly with IR, UV, and ESR spectroscopy.

Triplet vinylnitrenes differ from aryl- and alkylnitrenes in their reactivity. We have shown that triplet sensitization of vinyl azides can be used to form triplet vinylnitrenes.[17] Owing to their significant 1,3-biradical character, triplet vinylnitrenes are flexible and can rotate around their vinylic bond (Scheme 3). Triplet vinylnitrenes are short-lived in comparison with triplet aryl- and alkylnitrenes because their flexibility facilitates intersystem crossing to form products, rather than undergoing

Received: June 5, 2016
Published: October 22, 2016

DOI: 10.1021/jacs.6b05746
J. Am. Chem. Soc. 2016, 138, 14905−14914

Scheme 1. Reactivity of Singlet and Triplet Arylnitrenes

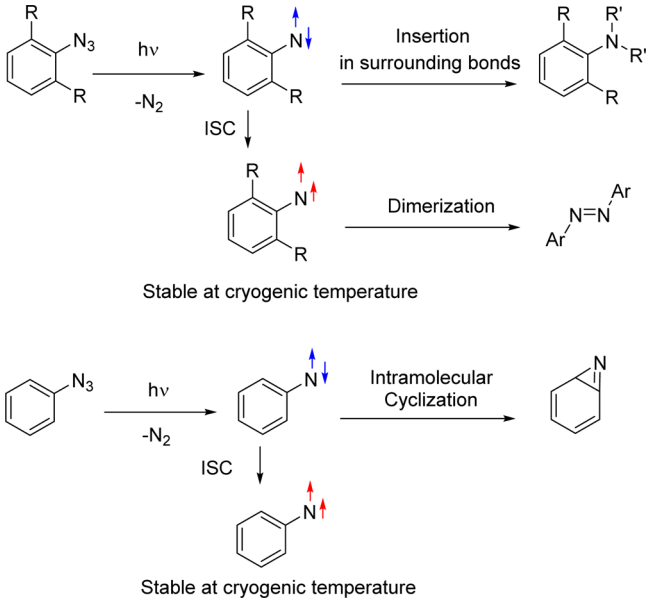

Scheme 2. Reactivity of Triplet Alkylnitrenes

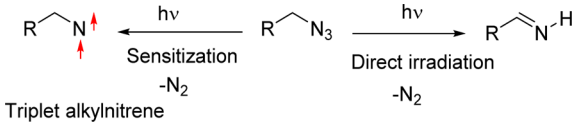

Scheme 3. Reactivity of Triplet Vinylnitrenes

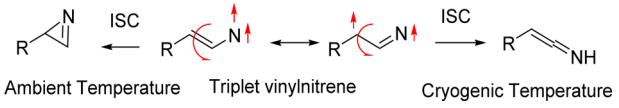

decay by dimerization.[17−20] However, structural rigidity in vinylnitrenes can render them stable at cryogenic temperatures.[21]

In this Article, we describe how molecular structure can be used to further control the stability and reactivity of vinylnitrenes. We studied the photoreactivity of vinyl azide **1**, which has a built-in triplet sensitizer and forms triplet vinylnitrene ^{3}**2** upon irradiation. Because vinylnitrene **2** is sterically strained, it does not decay by intersystem crossing to form an azirine, but rather it selectively forms heterocyclic dimer **3**. Furthermore, because vinyl azide **1** absorbs visible light, irradiation with a 405 nm diode can be used for quantitative transformation of vinyl azide **1**, via vinylnitrene ^{3}**2**, to dimer **3**. We used matrix isolation, ESR spectroscopy, laser flash photolysis, and calculations to elucidate the reaction mechanism for forming vinylnitrene ^{3}**2** and to aid in characterizing its physical properties.

RESULTS

Product Studies. Photolysis of **1** with a 405 nm LED allowed for selective formation of heterocyclic dimer **3** (Figure 1A). Similarly, irradiation of vinyl azide **1** in argon-saturated chloroform-d_3 with a mercury arc lamp through a Pyrex filter, monitored with ^{1}H NMR and IR spectroscopy, demonstrated that **1** forms heterocyclic dimer **3** selectively (Figure 1B).

We propose that heterocyclic dimer **3** is formed by dimerization of vinylnitrene ^{3}**2**, followed by autoxidation

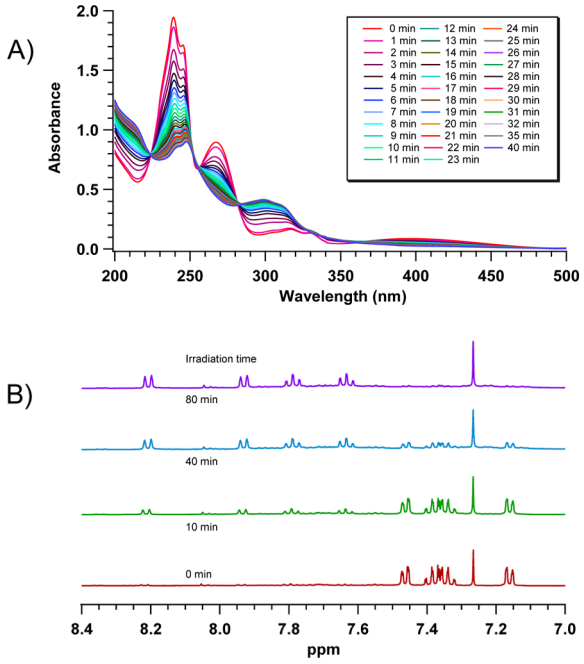

Figure 1. Photolysis of vinyl azide **1** (A) in acetonitrile with 405 nm irradiation and followed by UV−vis spectroscopy, and (B) in chloroform-d_3 with mercury arc lamp irradiation through Pyrex followed by ^{1}H NMR spectroscopy.

(Scheme 4). In more detail, we theorize that irradiation of vinyl azide **1** yields its first singlet excited state (S_1 of **1**), which

Scheme 4. Proposed Mechanism for Forming Heterocyclic Dimer 3 from Vinyl Azide 1

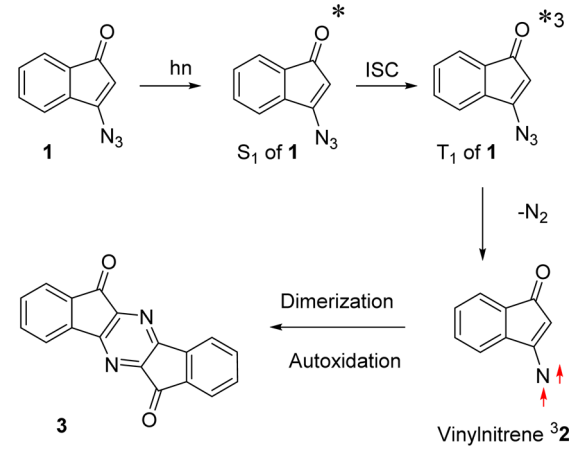

intersystem crosses to the triplet configuration (T_1 of **1**), and subsequently an N_2 molecule is extruded to form vinylnitrene ^{3}**2**. Thus, vinylnitrene ^{3}**2** is sufficiently stable to dimerize and not decay by intramolecular rearrangement.

Matrix IR Spectroscopy. Experiments were carried out in argon matrices to verify that irradiation of vinyl azide **1** results in formation of vinylnitrene ^{3}**2**. Azide **1** was deposited into an argon matrix at 20 K by gently heating it to 40 °C while using argon to entrain the vapor. Irradiating **1** in the Ar matrix through a 360−440 nm filter resulted in almost full depletion of the IR bands at 2122, 1724, 1557, 1376, and 1303 cm^{-1}, along with the formation of several new bands, including significant ones at 1669 and 1218 cm^{-1} (Figure 2A). These bands are

DOI: 10.1021/jacs.6b05746
J. Am. Chem. Soc. 2016, 138, 14905−14914

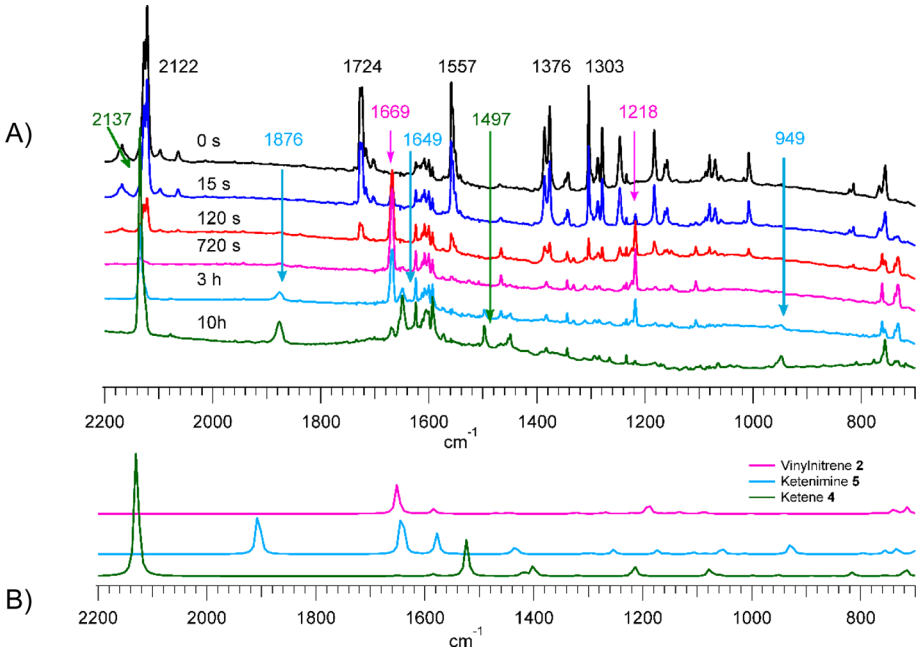

Figure 2. (A) IR spectra obtained before and after irradiation of vinyl azide **1** in an argon matrix at 10 K. (B) Calculated IR spectra of vinylnitrene ^{3}**2**, ketene **4**, and ketenimine **5**.

assigned to triplet vinylnitrene ^{3}**2** based on comparison with its calculated IR spectrum (Figure 2B), which places the most intense bands at 1714 (calculated intensity (i) = 573) and 1235 (i = 91) cm^{-1}. After scaling by 0.9613,[22] these bands are located at 1648 and 1187 cm^{-1}, which is in good agreement with the observed IR spectrum.

Further irradiation resulted in depletion of the IR bands of vinylnitrene ^{3}**2** with simultaneous formation of new bands, including significant ones at 2137, 1876, 1649, 1497, and 949 cm^{-1}. These new bands are assigned to ketene **4** and ketenimine **5** (Scheme 5) based on comparison with their

Scheme 5. Proposed Mechanism for Forming 4 and 5 from Vinylnitrene ^{3}2

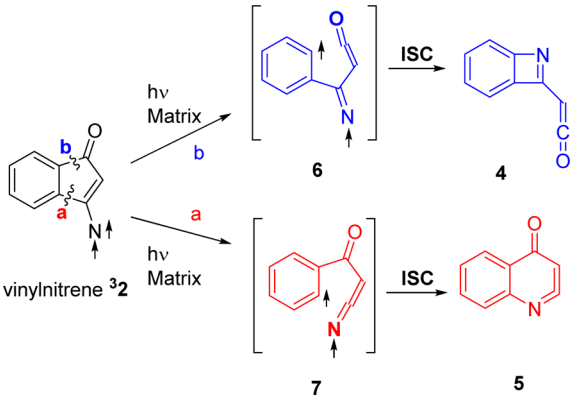

calculated IR spectra. The bands at 2137 and 1497 cm^{-1} are assigned to **4** because its calculated IR spectrum has the most intense bands at 2214 (i = 1336) and 1569 (i = 306) cm^{-1}, which after scaling are located at 2128 and 1508 cm^{-1}. The bands at 1876, 1649, and 949 cm^{-1} are assigned to **5**, as it has the most intense calculated bands at 1978 (i = 400), 1705 (i = 412), and 963 (i = 102) cm^{-1}, which after scaling are located at 1901, 1639, and 926 cm^{-1}. The calculated bands for both **4** and **5** are in good agreement with the experimental bands.

The matrix isolation shows that vinylnitrene ^{3}**2** is formed selectively at cryogenic temperature and is stable, but further irradiation cleaves its Ar−C bonds to yield ketene **4** and ketenimine **5**, as shown in Scheme 5.

ESR Spectroscopy. We used electron spin resonance (ESR) spectroscopy to determine the significance of the 1,3-biradical character of vinylnitrene ^{3}**2** (Scheme 6). Vinyl azide **1**

Scheme 6. 1,3-Biradical Character of Vinylnitrene ^{3}2

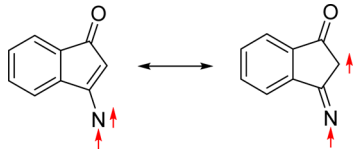

was dissolved in 2-methyltetrahydrofuran (MTHF), and the resulting solution was saturated with nitrogen and cooled to 80 K. The resulting matrix was irradiated for 120 s through a 360−440 nm filter, and the ESR spectrum was recorded between 4000 and 7000 G (Figure 3). The spectrum showed H_x and H_y lines at 4970 and 5567 G, and the zero-field splitting (zfs) parameters D and E for vinylnitrene ^{3}**2** were calculated to be D/hc = 0.460 cm^{-1} and E/hc = 0.015 cm^{-1} using the Wasserman equation.[23] As the D parameter is inversely proportional to the distance between the two spin centers, the low D value for vinylnitrene ^{3}**2** corresponds to higher delocalization of the radical centers. Therefore, it can be concluded that vinylnitrene ^{3}**2** has significant 1,3-biradical character (Scheme 6).[21,24,25] Furthermore, the E value is an indicator for the symmetry of the spins, and because it is larger than 0.01 cm^{-1}, the spins in vinylnitrene ^{3}**2** are highly asymmetrical. The ESR spectrum verifies that vinylnitrene ^{3}**2** truly is a vinylic nitrene.

DOI: 10.1021/jacs.6b05746
J. Am. Chem. Soc. 2016, 138, 14905−14914

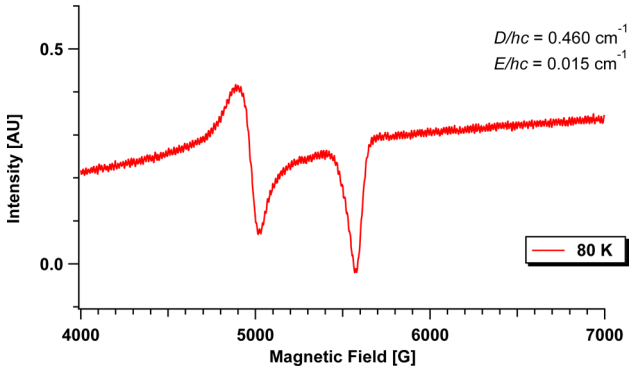

Figure 3. ESR spectrum of vinylnitrene ^{3}**2** in a glassy MTHF matrix at 80 K.

Transient Absorption Spectroscopy. We performed laser flash photolysis to identify the intermediates and excited states formed upon excitation of vinyl azide **1** in solution. Laser flash photolysis of **1** in argon-saturated acetonitrile showed a broad transient absorption from 300 to 520 nm with λ_{max} at ~340 and 480 nm (Figure 4). This absorption spectrum is

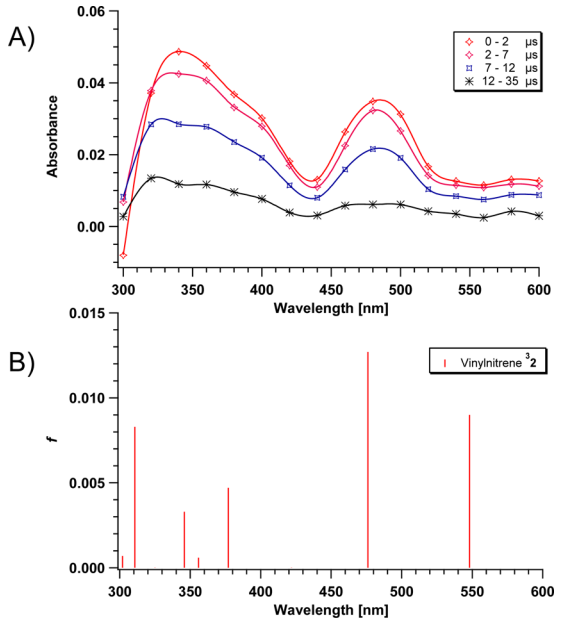

Figure 4. (A) Transient absorption of ^{3}**2** in argon-saturated acetonitrile, and (B) calculated electronic transitions (TD-DFT/B3LYP/6-31+G(d)) of vinylnitrene ^{3}**2**.

assigned to vinylnitrene ^{3}**2** based on similarities to the calculated spectrum. Time-dependent density functional theory (TD-DFT) calculations placed the major electronic transitions for vinylnitrene ^{3}**2** above 300 nm at 302 (f = 0.0007), 311 (f = 0.0083), 346 (f = 0.0033), 356 (f = 0.0006), 377 (f = 0.0047), 476 (f = 0.0127), and 548 nm (f = 0.0090), which fit with the observed spectrum.

The absorptions at 340 and 480 nm have the same kinetic profile, as they are both due to vinylnitrene ^{3}**2**. At 340 nm in argon-saturated acetonitrile, vinylnitrene ^{3}**2** is formed with a rate constant of 1.5×10^7 s^{-1} (τ = 67 ns) from its precursor, T_1 of **1**. The rate of decay of vinylnitrene ^{3}**2** depends on the concentration and the laser power (Figure 5). In oxygen-saturated acetonitrile, the absorption is completely quenched,

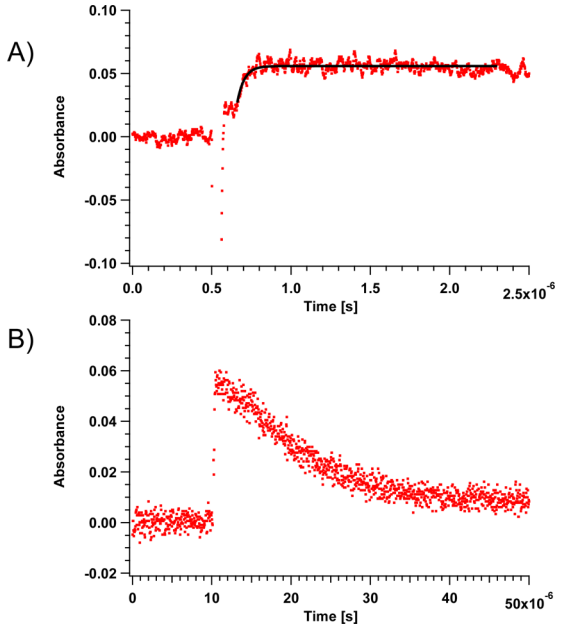

Figure 5. Kinetic traces at 340 nm obtained from laser flash photolysis of vinyl azide **1** in argon-saturated acetonitrile. (A) Formation and (B) decay of vinylnitrene ^{3}**2**.

as T_1 of **1** is efficiently quenched by oxygen, whereas in air-saturated solution, the decay rate constant is 3.2×10^6 s^{-1}. As the concentration of oxygen has been estimated to be 1.9×10^{-3} M in air-saturated acetonitrile,[26] the reaction rate between vinylnitrene ^{3}**2** and oxygen is estimated to be 1.7×10^9 M^{-1} s^{-1}. Vinylnitrene ^{3}**2** reacts efficiently with oxygen, which is similar to the reactivity reported for other triplet vinylnitrenes, owing to its significant 1,3-biradical character.[18−20]

To further characterize the properties of vinylnitrene ^{3}**2**, its reactivity with isoprene was determined using laser flash photolysis. The yield of the absorption at 340 nm decreases with increased isoprene concentration, verifying that vinylnitrene ^{3}**2** is formed from a triplet precursor, T_1 of **1**, and not by intersystem crossing from its singlet configuration (see the Stern−Volmer graph in Figure S11 in the Supporting Information). Furthermore, with increased isoprene concentration, the rate constant for the pseudo-first-order decay of the absorption at 340 nm increased (Figure 6A). A plot of the decay rate constant of vinylnitrene ^{3}**2** versus the concentration of isoprene yields a straight line with a slope of 2×10^6 M^{-1} s^{-1}, which is the rate for direct reaction of isoprene with vinylnitrene ^{3}**2** (Figure 6B). Thus, vinylnitrene ^{3}**2** can be trapped directly by bimolecular reaction with isoprene. The adducts formed between vinylnitrene ^{3}**2** and isoprene were isolated and characterized as **8** and **9**. The proposed mechanism for their formation is displayed in Scheme 7.

Because the decay rate for vinylnitrene ^{3}**2** depends on the laser power, they must decay by reacting with another nitrene molecule. However, because vinylnitrene ^{3}**2** reacts with isoprene, it is reasonable to assume that vinylnitrene ^{3}**2** can also react with its precursor, vinyl azide **1**, and this decay pathway may depend on the concentration.

UV−Vis Absorption Spectroscopy. To correlate the spectroscopic characterization of vinylnitrene ^{3}**2** in cryogenic matrices and in solution at ambient temperature, we obtained UV−vis spectra of vinylnitrene ^{3}**2** in a glassy MTHF matrix at 84 K. A solution of 0.20 mM of **1** in MTHF was bubbled with

DOI: 10.1021/jacs.6b05746
J. Am. Chem. Soc. 2016, 138, 14905−14914

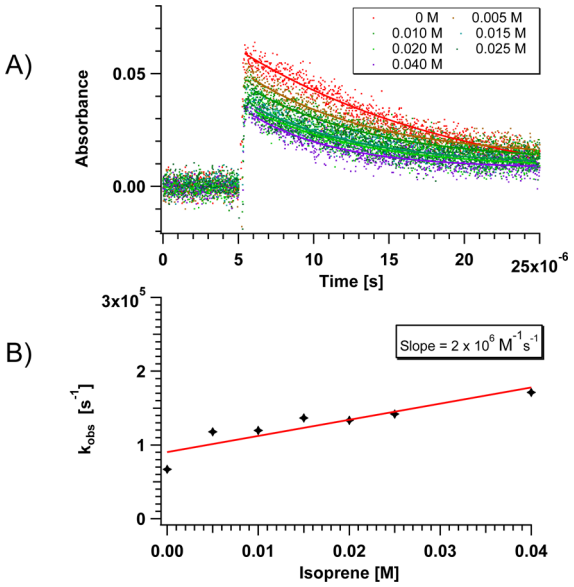

Figure 6. (A) Kinetic traces obtained at 340 nm for various isoprene concentrations in argon-saturated acetonitrile. (B) Rate constant for the decay (k_{obs}) at 340 nm as a function of isoprene concentration.

Scheme 7. Proposed Mechanisms for Trapping Vinylnitrene ^{3}2 with Isoprene to form 8 and 9

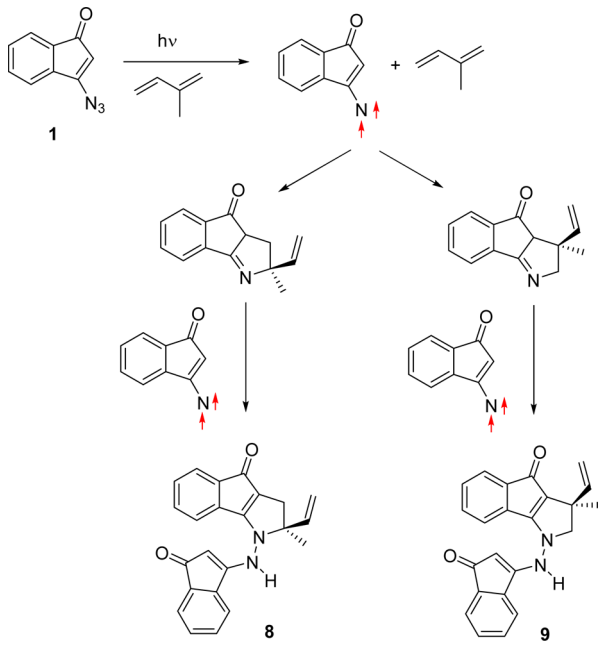

N_2 for 10 min and sealed. The ground state (S_0) UV−vis absorption spectrum of this solution at 293 K showed broad absorption between 330 and 475 nm with λ_{max} at 320 and 400 nm (Supporting Information, Figure S4). The solution was then cooled to 84 K using liquid nitrogen. Irradiation of **1** in the glassy MTHF matrix at 84 K with 405 ± 5 nm light (500 W xenon lamp) resulted in the formation of an absorption peak at ∼340 nm and broad absorption between 460 and 600 nm, with λ_{max} at ∼340 and ∼490 nm. With increased irradiation time, the intensity of the new bands increased (Figure 7), whereas the absorbance due to vinyl azide **1** decreased. The depletion of the starting material results in a negative absorption band with λ_{max} at ∼320 and ∼415 nm. The absorption bands at ∼340 and

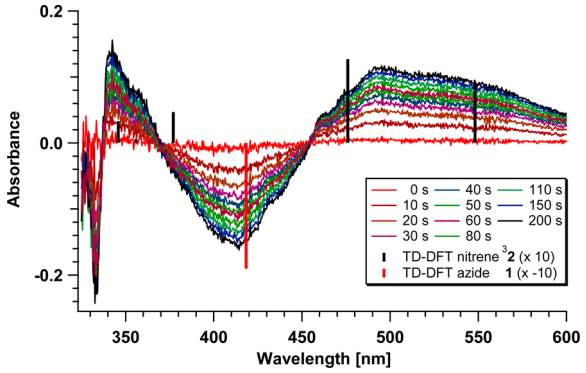

Figure 7. UV−vis difference spectra obtained by photolysis of vinyl azide **1** in glassy MTHF at 84 K, and TD-DFT calculated electronic transitions for vinyl azide **1** (red, intensities multiplied by −10) and vinylnitrene ^{3}**2** (black, intensities multiplied by 10).

∼490 nm match the bands observed in the transient absorption spectra of vinylnitrene ^{3}**2** obtained by laser flash photolysis of vinyl azide **1** (Figure 4). Therefore, we conclude that photolysis of vinyl azide **1** at ambient temperature and in glassy matrices at 84 K both result in the formation of vinylnitrene ^{3}**2**.

Quantum Chemical Calculations. Density functional theory (DFT) calculations were performed to support the proposed reaction mechanism for the formation of vinylnitrene ^{3}**2** from **1**, using Gaussian09[27] at the B3LYP level of theory with the 6-31+G(d) basis set.[28,29] We optimized S_0 of **1** and performed TD-DFT calculations[22,30,31] to locate the vertical excitation energy of S_1 of **1**, which was placed at 68 kcal/mol above its S_0, whereas T_1 and T_2 of **1** were located at 45 and 58 kcal/mol, respectively (Figures 8 and 9, Table 1).

In comparison, the optimized structure of T_1 of **1** is 40 kcal/mol above its S_0, which is a slightly lower energy than that obtained from the TD-DFT calculation, which must be due to the different geometries of S_0 and T_1 of **1**. The vinyl C−C bond

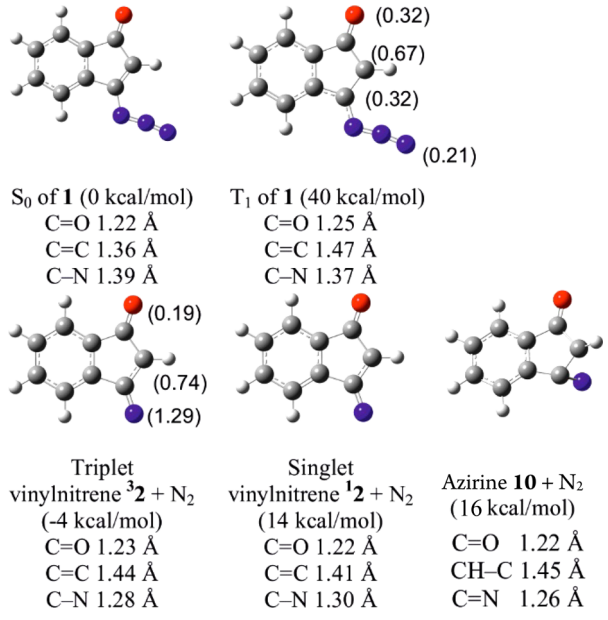

Figure 8. Optimized structures of **1**, T_1 of **1**, triplet vinylnitrene ^{3}**2**, singlet vinylnitrene ^{1}**2**, and azirine **10**. Calculated bond lengths, spin densities (in parentheses), and relative energies obtained from DFT calculations are shown.

DOI: 10.1021/jacs.6b05746
J. Am. Chem. Soc. 2016, 138, 14905−14914

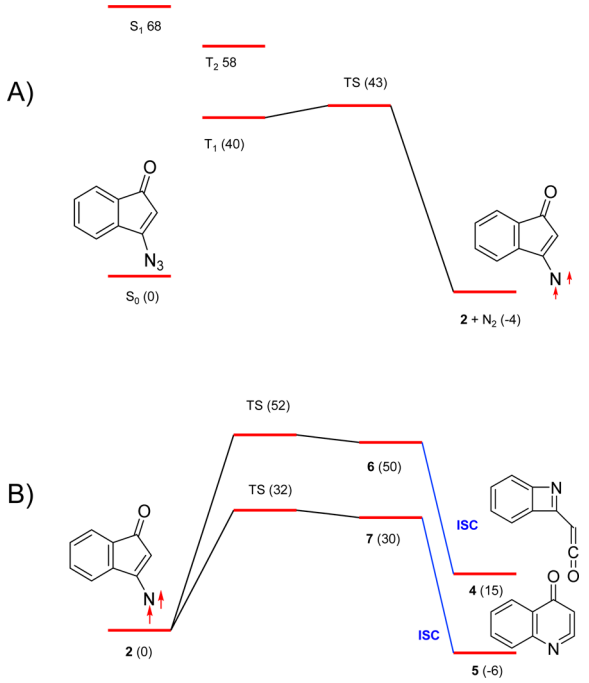

Figure 9. (A) Calculated stationary points on the triplet energy surface of vinyl azide **1**. (B) Calculated stationary points on the energy surface of triplet vinylnitrene ^{3}**2**. Energies are in kcal/mol. The energies of S_1 (68) and T_2 (58) of **1** were obtained from TD-DFT calculations, whereas the energies of S_0 (0), ^{3}**2**, and TSs, **4**–**7**, were obtained from optimization calculations.

is elongated in T_1 of **1** (1.47 Å) in comparison with its S_0, which indicates that T_1 of **1** has a (π,π*) configuration. This assignment is further supported by spin density calculations, which demonstrate that the spin densities are mainly located on the α-C (0.67) and β-C (0.32) atoms, as well as the oxygen atom of T_1 of **1** (0.32, Figure 8).

Optimization of vinylnitrene ^{3}**2** reveals that its C–N bond is somewhat shorter than the C–N bond in S_0 of **1**, indicating that it has a double bond character, and thus vinylnitrene ^{3}**2** has significant 1,3-biradical character. As the calculated spin densities are mainly located on the nitrogen atom (1.29) and the α-C atom (0.74), with a smaller spin density on the oxygen atom (0.19), the calculations further support that vinylnitrene ^{3}**2** has significant 1,3-biradical character (Figure 8). The open-shell singlet vinylnitrene ^{1}**2** was optimized using the broken symmetry method, as described in the literature.[32,33] The broken symmetry calculations were achieved using guess = mix as a keyword in Gaussian09, and they yielded vinylnitrene ^{1}**2** with a total spin ($\langle S^2 \rangle$) value of 1.01. Such an $\langle S^2 \rangle$ value is typical of 50:50 wave functions, which have significant spin contamination from the triplet state. Singlet vinylnitrene ^{1}**2** is 17.5 kcal/mol higher in energy than the triplet vinylnitrene, and this singlet–triplet energy gap (ΔE_{ST}) is similar to those obtained for several other vinylnitrenes using the same calculation methods.[17,18,20] Due to the high degree of spin contamination in the singlet, however, the DFT-calculated energy gap is considered less reliable than that obtained with CASPT2 (vide infra).

The calculated stationary points on the energy diagram for forming vinylnitrene ^{3}**2** from azide **1** are displayed in Figure 9A. The calculated transition state to form vinylnitrene ^{3}**2** from T_1 of **1** is 3 kcal/mol above T_1 of **1**. This diagram highlights that the extrusion of a nitrogen molecule from T_1 of **1** to produce vinylnitrene ^{3}**2** is facile. Interestingly, the optimized structure of azirine **10** is located 16 kcal/mol above vinylnitrene ^{3}**2**, which nicely explains why vinylnitrene ^{3}**2** does not decay by intersystem crossing to form azirine **10**.

The calculated energy diagram for the formation of ketene **4** and ketenimine **5** from vinylnitrene ^{3}**2** is displayed in Figure 9B. The transition states to form radical intermediates **6** and **7** are located 52 and 32 kcal/mol above vinylnitrene ^{3}**2**, respectively, thus implying that products **4** and **5** are both formed photochemically.

To better estimate the energy gap between the singlet and triplet configurations of vinylnitrene **2**, we performed CASSCF and CASPT2 calculations,[34,35] using the cc-pVDZ basis set[36] and a 12-electron, 12-orbital active space. The geometries of the different spin states were optimized at the CASSCF-(12,12)/cc-pVDZ level, and single-point energies were computed at the CASPT2(12,12)/cc-pVDZ level. For comparison, we performed similar calculations on the singlet and triplet states of vinylnitrene **11** (Table S1), using a 14-electron, 14-orbital active space. The CASSCF and CASPT2 calculations were performed with MOLCAS.[37]

The CASPT2 calculations place the triplet state of vinylnitrene **2** 10 and 44 kcal/mol below its open- and closed-shell singlet states, respectively. The CASSCF and CASPT2 calculations indicate that the DFT calculations overestimate the energy gap between the lowest singlet and triplet configurations of vinylnitrene **2** by ~7 kcal/mol. Thus, the energy gap is significantly smaller than that observed for phenylnitrene (14.9 kcal/mol),[38,39] but similar to what Wenthold calculated for 2-furanylnitrene, which has an unusually small singlet–triplet energy gap of 10.9 kcal/mol.[40] The author explained that the furanyl moiety is better able to stabilize the singlet configuration of 2-furanylnitrene than its triplet. Thus, we propose that similar factors affect the singlet–triplet splitting in vinylnitrene ^{3}**2**.

DISCUSSION

With irradiation at wavelengths greater than 300 nm, the ketone chromophore of vinyl azide **1** is selectively excited to yield S_1 of **1**, which has a (π,π*) configuration. Subsequently, S_1 of **1** undergoes efficient intersystem crossing to T_1 of **1**, which

Table 1. B3LYP, CASSCF, and CASPT2 Results for Vinylnitrene ^{3}2[a]

	B3LYP/6-31+G*			CASSCF(12,12)/cc-pVDZ		CASPT2(12,12)/cc-pVDZ// CASSCF(12,12)/cc-pVDZ	
state	*E* (au)	$\langle S^2 \rangle$	rel E	*E* (au)	rel *E*	*E* (au)	rel *E*
^{3}A″	−475.86468	2.05	0.0	−473.15532	0.0	−474.44374	0.0
^{1}A″	−475.83674	1.01	17.5	−473.13889	10.3	−474.42771	10.1
^{1}A′	−475.81012		34.2	−473.07723	49.0	−474.37330	44.2

[a]Relative energies in kcal/mol, not corrected for ZPE difference.

DOI: 10.1021/jacs.6b05746
J. Am. Chem. Soc. 2016, 138, 14905–14914

extrudes a N_2 molecule to form vinylnitrene ^{3}**2**. Because vinylnitrene ^{3}**2** is stable at cryogenic temperature, it was characterized directly with UV, ESR, and IR spectroscopy. The D/hc value obtained from the ESR spectrum of vinylnitrene ^{3}**2** indicates that the two unpaired electrons are highly delocalized on the nitrogen atom and the vinylic carbon atom, and this is also indicated by the spin density calculations (Figure 8). The D/hc value measured for vinylnitrene ^{3}**2** is similar to those observed for vinylnitrenes such as 3-aza-4-cyano-1,3-butadienylnitrene, 4-aza-4-cyano-1,3-butadienylnitrene, and 4-cyano-1,3-butadienylnitrene, which acquire delocalization through extended conjugation.[24] However, vinylnitrene ^{3}**2** is different, as it is not as highly conjugated, and thus we propose that the steric demand of the five-membered ring is better accommodated by elongation of the vinyl bond, which results in further delocalization of the spin density over the C═C−N chromophore. Wentrup and co-workers have shown that there is a linear correlation between the D/hc value and the calculated natural spin density on the nitrogen atom in nitrenes, and vinylnitrene ^{3}**2** follows the same trend.[41]

Although vinylnitrene ^{3}**2** has significant 1,3-biradical character, its vinyl bond is not flexible because it is part of a cyclic structure. This restriction of rotation around the vinyl bond is the key factor for rendering vinylnitrene ^{3}**2** stable at cryogenic temperature. Acyclic triplet vinylnitrenes, which have small rotational barriers around their vinyl bonds due to their 1,3-biradical character, are not observed in cryogenic matrices because they intersystem cross to ketenimine products (Scheme 8).[19,20] Thus, intersystem crossing in vinylnitrenes is facilitated by rotation around their vinyl bonds.

Scheme 8. Reactivity of Triplet Vinylnitrenes ^{3}12 and ^{3}13 in Argon Matrices

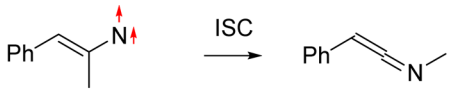

Vinylnitrene ^{3}**12**

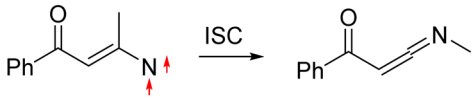

Vinylnitrene ^{3}**13**

We have previously shown that vinylnitrene ^{3}**11** (Scheme 9), which is part of a cyclic structure, is also stable at cryogenic temperature.[21] However, there is a significant difference between the physical properties of vinylnitrenes ^{3}**2** and ^{3}**11**, and their reactivities. Vinylnitrene ^{3}**11** does not yield isolatable products in solution at ambient temperature, just tar, presumably because it decays by intersystem crossing to form the corresponding azirine, which is not stable and polymerizes.

Banert and co-workers have also demonstrated that steric strain affects the reactivity of cyclic vinyl azides.[42,43] For example, they showed that photolysis of vinyl azide **14** yields azirine **15**, whereas steric strain prevents vinyl azide **16** from forming the corresponding azirine, and instead it forms bimolecular products **17** and **18** (Scheme 10). It was theorized that these products result from a triplet vinylnitrene intermediate.

Scheme 9. Comparison of the Zero-Field Splitting (zfs) Parameters D and E for Vinylnitrenes ^{3}2 and ^{3}11 and Calculated S−T Energy Gaps

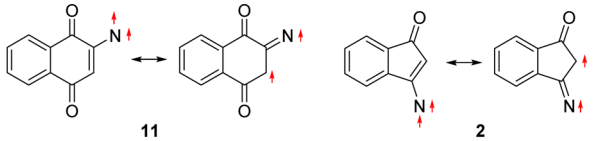

11 **2**

zfs parameters		
D/hc	0.7292 cm^{-1}	0.460 cm^{-1}
E/hc	0.0048 cm^{-1}	0.015 cm^{-1}
S-T energy gap (kcal/mol)		
B3LYP	16.1	17.5
CASSCF	16.4	10.3
CASPT	13.0	10.1

Scheme 10. Photoproducts Obtained from Cyclic Vinyl Azides 14 and 16

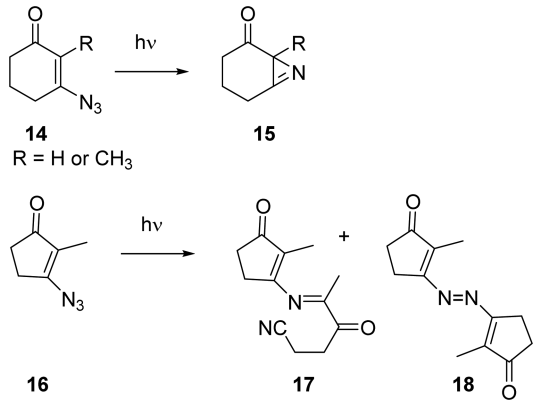

The zero-field splitting parameters for vinylnitrenes ^{3}**2** and ^{3}**11** (Scheme 9) clearly demonstrate that vinylnitrene ^{3}**2** has more significant 1,3-biradical character than that of vinylnitrene ^{3}**11**, owing to the steric demand of the five-membered ring. Furthermore, the steric demand of the five-member ring in vinylnitrene ^{3}**2** prevents it from decaying by intersystem crossing in solution to form azirine **10**. We theorize that vinylnitrene ^{3}**2** dimerizes in a stepwise manner to form a biradical that then rotates to acquire the necessary conformation to be able to intersystem cross to form product. Because vinylnitrene ^{3}**2** has significant 1,3-biradical character, it instead dimerizes to form new C−N bonds. Thus, the molecular structure of vinylnitrene ^{3}**2** allows it to be used to make heterocyclic dimers, which have found use in material sciences.[44]

Interestingly, the CASPT2 calculated singlet−triplet energy gap for vinylnitrene **2** is only 10 kcal/mol, which is smaller than that calculated for vinylnitrene ^{3}**11** of 13 kcal/mol using the same method. However, both these triplet vinylnitrenes are stable at cryogenic temperature; thus, the energy gap between their singlet and triplet configurations is not the major driving force for their different reactivities.

■ CONCLUSION

In conclusion, we have successfully constructed a triplet vinylnitrene that decays by dimerization at ambient temper-

DOI: 10.1021/jacs.6b05746
J. Am. Chem. Soc. 2016, 138, 14905−14914

ature. The steric strain of the five-membered ring molecular architecture of the vinylnitrene prevents decay by unimolecular rearrangement. Instead, the vinylnitrene dimerizes, similar to other triplet nitrenes that are stabilized by electron-donating groups. However, due to the significant 1,3-biradical character of vinylnitrene ^{3}**2**, it dimerizes to form not a N−N bond, but rather a C−N bond. Thus, with smart molecular architecture vinylnitrenes have the potential to be used in synthetic applications to make new C−N bonds.

EXPERIMENTAL SECTION

Matrix IR Spectroscopy. Argon was deposited at 20 K for 5 min on a CsI target inside the cryostat cold head. The sample was then sublimed at 40 °C and deposited with argon at 20 K for 40 min in the vacuum of a diffusion pump. The cryostat cold head was cooled to 10 K for sample irradiation. The argon matrix containing the deposited molecules of **1** was irradiated through quartz windows using a 360−440 nm filter and IR spectra were recorded after various irradiation times.

ESR Spectroscopy. A 0.20 mM solution of 1 in anhydrous MTHF was degassed with nitrogen for 10 min. After degassing through a rubber septum, the tube containing the solution was sealed with parafilm and used for ESR spectroscopy measurements.

Quantum Chemical Calculations. All the geometries were optimized at the B3LYP level of theory and with the 6-31+G(d) basis set, as implemented in the Gaussian09 programs.[27−29] The absorption spectra were calculated using time-dependent density functional theory (TD-DFT).[30,31,45] All transition states were confirmed to have one imaginary vibrational frequency by the analytical determination of the second derivative of the energy with respect to the internal coordinates. Intrinsic reaction coordinate calculations were used to verify that the transition state correlates with the products and the triplet excited state of the starting material.[46,47] All DFT calculations were performed at the Ohio Supercomputer Center. CASSCF and CASPT2 calculations[34,35] on nitrene **2** used the cc-pVDZ basis set[36] and a 12-electron, 12-orbital active space consisting of all π and π^* MOs, plus the in-plane nonbonding orbital on nitrogen. Single-point energies were computed at the CASPT2-(12,12)/cc-pVDZ level at the CASSCF(12,12)/cc-pVDZ geometries. The CASSCF and CASPT2 calculations were performed with MOLCAS.[37]

Laser Flash Photolysis. Laser flash photolysis experiments were carried out with an excimer laser (308 nm, 17 ns).[48] A stock solution of azide **1** in acetonitrile was prepared with an absorbance at 308 nm of 0.3−0.8. Quartz cuvettes with a 10 mm × 10 mm cross section were used. For each kinetic trace approximately 2 mL of the stock solutions was placed in the cuvette. The solution was degassed with argon for about 5 min prior to the experiment. The kinetic traces were fitted using Igor Pro software.

Preparation of 1. *Synthesis of 3-Bromo-1-indenone.* In a 100 mL round bottomed flask, 1-indanone (0.500 g, 3.788 mmol) was dissolved in 20 mL of carbon tetrachloride, and *N*-bromosuccinimide (1.353 g, 7.601 mmol) and a catalytic amount of AIBN (11.000 mg, 0.067 mmol) were added to the solution. The resulting solution was illuminated using visible light (75 W) under refluxing conditions for 2 h. Following cooling to 0 °C, triethylamine (1.340 g, 13.267 mmol) was added and the reaction mixture was stirred for another 9 h. The solids were removed from the reaction mixture by filtration and washed with carbon tetrachloride. The filtrate was concentrated and then diluted with 50 mL of diethyl ether, and the organic portion was extracted using 0.1 N HCl (50 mL). The organic layer was dried over magnesium sulfate and solvent was removed under reduced pressure to yield pure 3-bromo-1-indenone (0.752 g, 3.598 mmol, 95% yield). The product was characterized using ^{1}H NMR spectroscopy, and the data were in accordance with the literature.[49] ^{1}H NMR (400 MHz, $CDCl_3$): δ 7.48−7.46 (m, 1H), 7.44−7.42 (m, 1H), 7.36−7.33 (m, 1H), 7.22−7.20 (m, 1H), 6.22 (s, 1H) ppm; ^{13}C NMR (400 MHz, $CDCl_3$): 193.9, 148.6, 142.9, 133.6, 130.4, 130.3, 127.4, 121.9, 121.3 ppm; IR (neat): 3114, 1713, 1603, 1539, 1453, 1361, 1246, 1181, 1047, 765 cm^{-1}.

Synthesis of 3-Azido-1-indenone (1). 3-Bromo-1-indenone (0.338 g, 1.617 mmol) was dissolved in 30 mL of acetone in a 100 mL round bottomed flask. Sodium azide (0.126 g, 1.938 mmol) was then added to the solution in portions over 10 min. The resulting solution was stirred for 24 h for complete conversion, and then the acetone was removed. The residue was dissolved in 40 mL of diethyl ether and washed several times with water. The organic layers were combined and dried over magnesium sulfate. The organic solvent was removed under reduced pressure to obtain pure 3-azido-1-indenone (**1**) (0.260 g, 1.520 mmol, 94% yield). The product was characterized using ^{1}H and ^{13}C NMR spectroscopy. ^{1}H NMR (400 MHz, $CDCl_3$): δ 7.46−7.45 (m, 1H), 7.39−7.34 (m, 2H), 7.17−7.15 (m, 1H), 5.62 (s, 1H) ppm; ^{13}C NMR (400 MHz, $CDCl_3$): δ 193.5, 163.6, 139.5, 132.8, 132.4, 130.6, 122.0, 119.1, 108.5 ppm; IR (neat): 3070, 2167, 2124, 1706, 1548, 1373, 1299, 1280, 1244, 1184, 1081 cm^{-1}. HRMS: 144.0444 (exptl); 144.0445 (calcd $C_9H_5NO+H^+$).

Preparative Photolysis of 1. *Photolysis of Vinyl Azide 1 with High-Pressure Mercury Arc Lamp.* Vinyl azide **1** (0.100 g, 0.585 mmol) was dissolved in 15 mL of chloroform and then degassed by bubbling argon through the solution for 8 min. The resulting solution was photolyzed using a mercury lamp with a Pyrex filter for 90 min at room temperature, which resulted in complete consumption of the starting material and formation of dimer **3** (0.077 g, 0.271 mmol, 93% yield). Dimer **3** was characterized based on spectroscopic data. ^{1}H NMR (400 MHz, $CDCl_3$): δ 8.22−8.20 (m, 2H), 7.94−7.92 (m, 2H), 7.81−7.77 (m, 2H), 7.65−7.61 (m, 2H) ppm; ^{13}C NMR (400 MHz, $CDCl_3$): δ 187.4, 162.0, 142.3, 136.6, 134.9, 132.8, 126.5, 125.5, 122.5 ppm; IR (neat): 3067, 1729, 1628, 1602, 1550, 1385, 1276, 1084, 910, 724 cm^{-1}; HRMS: 285.0606 (exptl), 285.0664 (calcd $C_{18}H_8N_2O_2$).

Photolysis of Vinyl Azide 1 with 405 nm Diode. Vinyl azide **1** (2.0 mg, 0.012 mmol) was dissolved in 0.7 mL of chloroform-d_3 and then degassed by bubbling argon through the solution for 8 min. The resulting solution was irradiated with two 262 mA 405 nm diodes with an output of 200−260 mW at 350 mA. The progress of the reaction was followed by ^{1}H NMR spectroscopy, which revealed that, after 15 min of photolysis, vinyl azide **1** was fully depleted and the only product formed was dimer **3**.

Vinyl azide **1** (10 mg, 0.012 M) was dissolved in acetonitrile (5 mL) and irradiated with 405 nm LED diodes with a luminous flux of 100 mW and a forward current of 150 mA. Product formation was analyzed by UV−vis spectroscopy, and complete conversion took place within 20 min. UV photolysis was also repeated at a lower concentration of vinyl azide **1** (0.048 mM), which gave similar results.

Photolysis of Vinyl Azide 1 with Isoprene. Vinyl azide **1** (52 mg, 0.30 mmol) and isoprene (500 μL, 5 mmol) were dissolved in acetonitrile (8 mL), and then argon was bubbled through the solution for 10 min. The resulting solution was irradiated until ^{1}H NMR spectroscopy showed ∼30% remaining of the starting material. The photoproducts were separated on silica column eluted with 30% ethyl acetate in hexane to yield products **8** (13 mg, 0.037 mmol) and **9** (7 mg, 0.020 mmol) that were characterized with NMR, IR and MS spectroscopy. Compound **8**: ^{1}H NMR (400 MHz, $CDCl_3$): δ 7.94 (d, J = 8 Hz, 1H), 7.86 (d, J = 8 Hz, 1H), 7.8−7.7 (m, 2H), 7.58−7.62 (t, 8 Hz, 1H), 7.51−7.54 (m, 1H), 7.33−7.36 (m, 2H), 6.10 (s, 1H), 5.65−5.73, (dd, J = 6 and 11 Hz, 1H), 5.31 (d, J = 6 Hz, 1H), 4.87 (d, J = 11 Hz, 1H), 2.96 (d, J = 14 Hz, 1H), 2.52 (s, 1H), 2.17 (d, J = 14 Hz, 1H), 1.32 (s, 3H) ppm; ^{13}C NMR (400 MHz, $CDCl_3$): 194.7, 193.9, 156.6, 148.1, 142.0, 138.7, 137.3, 134.6, 133.3, 132.5, 131.1, 130.3, 126.3, 125.5, 125.2 121.4, 114.0, 106.0, 100.0, 90.4, 70.1, 44.1, 28.7 ppm; IR (neat): 3318, 2958, 2927, 2854, 1722, 1683, 1598, 1551, 1466, 1401, 1260, 1187, 1044, 1013, 959, 936, 886, 765, 686, 618, and 539 cm^{-1}; HRMS: 355.1438 (exptl), 355.1441 (calcd $C_{23}H_{18}N_2O_2+H^+$).

Compound 9. ^{1}H NMR (400 MHz, $CDCl_3$): δ 7.93 (d, 8 Hz, 1H), 7.91 (dd, 2 Hz, 6 Hz, 1H), 7.85 (d, J = 8 Hz, 1H), 7.77 (t, J = 8 Hz, 1H), 7.60 (t, J = 7 Hz, 1H), 7.54−7.52 (m, 1H), 7.40−7.34 (m, 2H), 6.01 (s, 1H), 5.75−5.68 (dd, J = 11 and 17 Hz, 1H), 4.92 (d, 17 J = Hz, 1H), 4.90 (d, J = 11 Hz, 1H), 2.72 (s, 1H), 2.63 (d, J = 14 Hz,

DOI: 10.1021/jacs.6b05746
J. Am. Chem. Soc. 2016, 138, 14905−14914

1H), 2.51 (d, J = 14 Hz, 1H), 1.21 (s, 3H) ppm; ^{13}C NMR (400 MHz, $CDCl_3$): 194.6, 194.0, 156.1, 148.5, 142.9, 138.7, 137.4, 135.0, 133.3, 132.5, 130.9, 130.4, 125.9, 125.5, 124.9, 121.5, 113.7, 105.8, 100.0, 89.5, 69.2, 44.9, 29.7 ppm; IR (neat): 3324, 2961, 2924, 2851, 1725, 1683, 1601, 1548, 1461, 1407, 1283, 1261, 1190, 1002, 917, 889, 762, 684, 616, 534, 514 cm^{-1}; HRMS: 355.1437 (exptl), 355.1441 (calcd $C_{23}H_{18}N_2O_2$+ H^+).

■ ASSOCIATED CONTENT

Supporting Information

The Supporting Information is available free of charge on the ACS Publications website at DOI: 10.1021/jacs.6b05746.

NMR and IR spectra of 3-bromo-1-indenone, **1, 3, 8** and **9**. UV−vis spectrum of **1**. Stern Volmer plot. Calculated structures of **1**−**7** and **10**-**11** (PDF)

■ AUTHOR INFORMATION

Corresponding Author

*anna.gudmundsdottir@uc.edu

Notes

The authors declare no competing financial interest.

■ ACKNOWLEDGMENTS

We thank the National Science Foundation (CHE-1464694 and CHE-1213425) and the Ohio Supercomputer Center for their generous support of this work. This work was also supported by a Grant-in-Aid for Science Research on Innovative Areas "Stimuli-responsive Chemical Species" from the Ministry of Education, Culture, Sports, Science and Technology, Japan. ESR measurements were performed at N-BARD, Hiroshima University

■ REFERENCES

(1) Bräse, S.; Gil, C.; Knepper, K.; Zimmermann, V. *Angew. Chem., Int. Ed.* **2005**, *44*, 5188−5240.

(2) *Organic Azides. Syntheses and Applications*;; Bräse, S., Banert, K., Eds.; John Wiley & Sons, Ltd.: Chichester, UK, 2010.

(3) Schultz, D. M.; Yoon, T. P. *Science* **2014**, *343*, 1239176.

(4) Farney, E. P.; Yoon, T. P. *Angew. Chem., Int. Ed.* **2014**, *53*, 793−797.

(5) Platz, M. S. Nitrenes. In *Reactive Intermediate Chemistry*; Moss, R. A., Platz, M. S., Jones, Jr., M., Eds.; John Wiley & Sons, Inc.: Hoboken, NJ, 2004.

(6) Muthukrishnan, S.; Ranaweera, R. A. A. U.; Gudmundsdottir, A. D. Triplet Alkyl Nitrenes. In *Nitrenes and Nitrenium Ions*; Falvey, D. E., Gudmundsdottir, A. D., Eds.; John Wiley & Sons, Inc.: Hoboken, NJ, 2013.

(7) Platz, M. S. *Photochem. Photobiol.* **1997**, *65*, 193−194.

(8) Cai, S. X.; Glenn, D. J.; Keana, J. F. W. *J. Org. Chem.* **1992**, *57*, 1299−1304.

(9) *Azides and Nitrenes. Reactivity and Utility*. Scriven, E. F. V., Ed. Academic Press Inc.: Orlando, FL, 1984.

(10) Niino, H.; Koga, Y.; Yabe, A. *J. Photochem. Photobiol., A* **1997**, *106*, 9−13.

(11) Mecomber, J. S.; Murthy, R. S.; Rajam, S.; Singh, P. N. D.; Gudmundsdottir, A. D.; Limbach, P. A. *Langmuir* **2008**, *24*, 3645−3653.

(12) Meijer, E. W.; Nijhuis, S.; Van Vroonhoven, F. C. B. M. *J. Am. Chem. Soc.* **1988**, *110*, 7209−7210.

(13) Kanakarajan, K.; Goodrich, R.; Young, M. J. T.; Soundararajan, S.; Platz, M. S. *J. Am. Chem. Soc.* **1988**, *110*, 6536−6541.

(14) Liang, T. Y.; Schuster, G. B. *J. Am. Chem. Soc.* **1987**, *109*, 7803−7810.

(15) Singh, P. N. D.; Mandel, S. M.; Sankaranarayanan, J.; Muthukrishnan, S.; Chang, M.; Robinson, R. M.; Lahti, P. M.; Ault, B. S.; Gudmundsdóttir, A. D. *J. Am. Chem. Soc.* **2007**, *129*, 16263−16272.

(16) Sankaranarayanan, J.; Bort, L. N.; Mandel, S. M.; Chen, P.; Krause, J. A.; Brooks, E. E.; Tsang, P.; Gudmundsdottir, A. D. *Org. Lett.* **2008**, *10*, 937−940.

(17) Rajam, S.; Jadhav, A. V.; Li, Q.; Sarkar, S. K.; Singh, P. N. D.; Rohr, A.; Pace, T. C. S.; Li, R.; Krause, J. A.; Bohne, C.; Ault, B. S.; Gudmundsdottir, A. D. *J. Org. Chem.* **2014**, *79*, 9325−9334.

(18) Gamage, D. W.; Li, Q.; Ranaweera, R. A. A. U.; Sarkar, S. K.; Weragoda, G. K.; Carr, P. L.; Gudmundsdottir, A. D. *J. Org. Chem.* **2013**, *78*, 11349−11356.

(19) Rajam, S.; Murthy, R. S.; Jadhav, A. V.; Li, Q.; Keller, C.; Carra, C.; Pace, T. C. S.; Bohne, C.; Ault, B. S.; Gudmundsdottir, A. D. *J. Org. Chem.* **2011**, *76*, 9934−9945.

(20) Zhang, X.; Sarkar, S. K.; Weragoda, G. K.; Rajam, S.; Ault, B. S.; Gudmundsdottir, A. D. *J. Org. Chem.* **2014**, *79*, 653−663.

(21) Sarkar, S. K.; Sawai, A.; Kanahara, K.; Wentrup, C.; Abe, M.; Gudmundsdottir, A. D. *J. Am. Chem. Soc.* **2015**, *137*, 4207−4214.

(22) Foresman, J. B.; Frisch, Æ. *Exploring Chemistry with Electronic Structure Methods*; Gaussian, Inc.: Pittsburgh, PA, 1996.

(23) Wasserman, E.; Snyder, L. C.; Yager, W. A. *J. Chem. Phys.* **1964**, *41*, 1763−1772.

(24) Wentrup, C.; Kvaskoff, D. *Aust. J. Chem.* **2013**, *66*, 286−296.

(25) Wentrup, C. *Acc. Chem. Res.* **2011**, *44* (6), 393−404.

(26) Clark, W. D. K.; Steel, C. *J. Am. Chem. Soc.* **1971**, *93*, 6347−6355.

(27) Frisch, M. J.; Trucks, G. W.; Schlegel, H. B.; Scuseria, G. E.; Robb, M. A.; Cheeseman, J. R.; Scalmani, G.; Barone, V.; Mennucci, B.; Petersson, G. A.; Nakatsuji, H.; Caricato, M.; Li, X.; Hratchian, H. P.; Izmaylov, A. F.; Bloino, J.; Zheng, G.; Sonnenberg, J. L.; Hada, M.; Ehara, M.; Toyota, K.; Fukuda, R.; Hasegawa, J.; Ishida, M.; Nakajima, T.; Honda, Y.; Kitao, O.; Nakai, H.; Vreven, T.; Montgomery, J. A., Jr.; Peralta, J. E.; Ogliaro, F.; Bearpark, M.; Heyd, J. J.; Brothers, E.; Kudin, K. N.; Staroverov, V. N.; Kobayashi, R.; Normand, J.; Raghavachari, K.; Rendell, A.; Burant, J. C.; Iyengar, S. S.; Tomasi, J.; Cossi, M.; Rega, N.; Millam, J. M.; Klene, M.; Knox, J. E.; Cross, J. B.; Bakken, V.; Adamo, C.; Jaramillo, J.; Gomperts, R.; Stratmann, R. E.; Yazyev, O.; Austin, A. J.; Cammi, R.; Pomelli, C.; Ochterski, J. W.; Martin, R. L.; Morokuma, K.; Zakrzewski, V. G.; Voth, G. A.; Salvador, P.; Dannenberg, J. J.; Dapprich, S.; Daniels, A. D.; Farkas, Ö.; Foresman, J. B.; Ortiz, J. V.; Cioslowski, J.; Fox, D. J. *Gaussian 09*, Revision B.01; Gaussian, Inc.: Wallingford, CT, 2009.

(28) Becke, A. D. *J. Chem. Phys.* **1993**, *98*, 5648−5652.

(29) Lee, C.; Yang, W.; Parr, R. G. *Phys. Rev. B: Condens. Matter Mater. Phys.* **1988**, *37*, 785−789.

(30) Bauernschmitt, R.; Ahlrichs, R. *Chem. Phys. Lett.* **1996**, *256*, 454−464.

(31) Foresman, J. B.; Head-Gordon, M.; Pople, J. A.; Frisch, M. J. *J. Phys. Chem.* **1992**, *96*, 135−149.

(32) Noodleman, L.; Baerends, E. J. *J. Am. Chem. Soc.* **1984**, *106*, 2316−2327.

(33) Yamaguchi, K.; Jensen, F.; Dorigo, A.; Houk, K. N. *Chem. Phys. Lett.* **1988**, *149*, 537−542.

(34) Andersson, K.; Malmqvist, P. A.; Roos, B. O.; Sadlej, A. J.; Wolinski, K. *J. Phys. Chem.* **1990**, *94*, 5483−5488.

(35) Andersson, K.; Malmqvist, P.-Å.; Roos, B. O. *J. Chem. Phys.* **1992**, *96*, 1218−1226.

(36) Dunning, T. H., Jr. *J. Chem. Phys.* **1989**, *90*, 1007−1023.

(37) Aquilante, F.; De Vico, L.; Ferré, N.; Ghigo, G.; Malmqvist, P.-å.; Neogrády, P.; Pedersen, T. B.; Pitoňák, M.; Reiher, M.; Roos, B. O.; Serrano-Andrés, L.; Urban, M.; Veryazov, V.; Lindh, R. *J. Comput. Chem.* **2010**, *31*, 224−247.

(38) Travers, M. J.; Cowles, D. C.; Clifford, E. P.; Ellison, G. B.; Engelking, P. C. *J. Chem. Phys.* **1999**, *111*, 5349−5360.

(39) Wijeratne, N. R.; Da Fonte, M.; Ronemus, A.; Wyss, P. J.; Tahmassebi, D.; Wenthold, P. G. *J. Phys. Chem. A* **2009**, *113*, 9467−9473.

(40) Wenthold, P. G. *J. Org. Chem.* **2012**, *77*, 208−214.

(41) Kvaskoff, D.; Bednarek, P.; George, L.; Waich, K.; Wentrup, C. *J. Org. Chem.* **2006**, *71*, 4049−4058.
(42) Banert, K.; Meier, B. *Angew. Chem., Int. Ed.* **2006**, *45*, 4015−4019.
(43) Banert, K.; Meier, B.; Penk, E.; Saha, B.; Wuerthwein, E.-U.; Grimme, S.; Rueffer, T.; Schaarschmidt, D.; Lang, H. *Chem. - Eur. J.* **2011**, *17*, 1128−1136.
(44) Nishida, J.-i.; Deno, H.; Ichimura, S.; Nakagawa, T.; Yamashita, Y. *J. Mater. Chem.* **2012**, *22*, 4483−4490.
(45) Stratmann, R. E.; Scuseria, G. E.; Frisch, M. J. *J. Chem. Phys.* **1998**, *109*, 8218−8224.
(46) Gonzalez, C.; Schlegel, H. B. *J. Chem. Phys.* **1989**, *90*, 2154−2161.
(47) Gonzalez, C.; Schlegel, H. B. *J. Phys. Chem.* **1990**, *94*, 5523−5527.
(48) Muthukrishnan, S.; Sankaranarayanan, J.; Klima, R. F.; Pace, T. C. S.; Bohne, C.; Gudmundsdottir, A. D. *Org. Lett.* **2009**, *11*, 2345−2348.
(49) Heffner, R. J.; Joullié, M. M. *Synth. Commun.* **1991**, *21*, 2231−22.

DOI: 10.1021/jacs.6b05746
J. Am. Chem. Soc. 2016, 138, 14905−14914